FINITE DIFFERENCE TIME DOMAIN IMPLEMENTATION OF SURFACE IMPEDANCE BOUNDARY CONDITIONS

by

John H. Beggs, Student Member, IEEE
Raymond J. Luebbers, Senior Member, IEEE
Kane S. Yee*, Member, IEEE
Karl S. Kunz, Senior Member, IEEE

Department of Electrical and Computer Engineering
The Pennsylvania State University
University Park, PA 16802

September 1990

Revised

September 1991

Revised

December 1991

* K. S. Yee is with the Lockheed Missiles and Space Company, Sunnyvale, California.

ABSTRACT

Surface impedance boundary conditions are employed to reduce the solution volume during the analysis of scattering from lossy dielectric objects. In a finite difference solution, they also can be utilized to avoid using small cells, made necessary by shorter wavelengths in conducting media throughout the solution volume. The standard approach is to approximate the surface impedance over a very small bandwidth by its value at the center frequency, and then use that result in the boundary condition. In this paper, two implementations of the surface impedance boundary condition are presented. One implementation is a constant surface impedance boundary condition and the other is a dispersive surface impedance boundary condition that is applicable over a very large frequency bandwidth and over a large range of conductivities. Frequency domain results are presented in one dimension for two conductivity values and are compared with exact results. Scattering width results from an infinite square cylinder are presented as a two dimensional demonstration. Extensions to three dimensions should be straightforward.

I. Introduction

The Finite Difference Time Domain (FDTD) technique permits the analysis of interactions of electromagnetic waves with objects of arbitrary shape and material composition. This method was first proposed by Yee [1] for isotropic, non-dispersive materials in 1966; and through various modifications during the past twenty years, it has evolved into a mature computational technique. Reference [2] and the references contained therein provide an account of various extensions and modifications of the original FDTD algorithm. The present FDTD technique is capable of electromagnetic scattering analysis from objects of arbitrary and complicated geometrical shape and material composition over a large band of frequencies. This technique has recently been extended to include dispersive dielectric materials [3], chiral materials [4] and plasmas [5]. Due to these numerous capabilities, the FDTD method has begun to gain widespread acceptance as a viable computational alternative to the classical method of moments (MM) technique for many problems.

To analyze electromagnetic field interaction with lossy dielectric objects, the FDTD method requires that the interior of the object be modeled in order for fields to penetrate the body. Accurate modeling often requires a very fine spatial grid resulting in a relatively large number of cells for moderately sized objects. A highly conducting dielectric object can be replaced by a surface impedance boundary condition (SIBC) that is a function of the material parameters. Thus, this boundary condition eliminates the spatial quantization of the object and reduces the overall size of the solution space not only by eliminating cells within the lossy dielectric, but also by allowing larger cells to be used in the

exterior region. As with any computational electromagnetic tool, a technique that reduces the solution space or number of unknowns is quite welcome.

Of historical interest, surface impedance boundary conditions were first proposed by Leontovich in the 1940's [6] and were rigorously developed by Senior in 1960 [7]. During the past thirty years, researchers have applied surface impedance concepts in the frequency domain to numerous electromagnetic scattering problems. Time domain surface impedance concepts received little attention until recently. Through some impressive work, Maloney and Smith [8] have previously implemented a surface impedance boundary condition in the FDTD method. However, their implementation has a minor disadvantage because the exponential rates and coefficients for recursive updating have to be reevaluated <u>each</u> time the conductivity or loss tangent is changed. With our proposed method, the exponential rates and coefficients only have to be evaluated <u>once</u>. Tesche [9] has also investigated surface impedance concepts in an integral equation time domain solution, but presented limited computational time domain results.

It is the purpose of this paper to introduce a constant surface impedance boundary condition that is applicable for a single frequency and a dispersive surface impedance boundary condition that is applicable over a large frequency bandwidth and range of conductivities. The dispersive surface impedance includes frequency variations which results in a time domain boundary condition involving a convolution. We will then show how to efficiently evaluate this convolved surface impedance using recursion.

II. Motivation

The motivation for implementing a SIBC in the FDTD method is to reduce the computational resource requirements for modeling highly conducting lossy dielectric objects. In the standard FDTD method, modeling highly conducting lossy dielectric objects requires that the cell size be chosen small enough to resolve the field <u>inside</u> the object at the maximum frequency of interest. For example, suppose scattering from a lossy dielectric object with permeability μ, permittivity ϵ and conductivity σ=2.0 S/m is to be studied over the frequency band 0-10 GHz. The cell size must be chosen as some fraction of the wavelength inside the conducting material at the maximum frequency of interest. Thus the cell size is chosen (typically) as

$$\delta x = \delta y = \delta z = \frac{\lambda}{10} = \frac{\lambda_0}{10\sqrt{|\hat{\epsilon}_r|}} \qquad (1)$$

where $\hat{\epsilon}_r$ is the complex relative permittivity constant of the material and λ and λ_0 are the wavelengths inside the material and in free space at 10 GHz, respectively. The complex permittivity for lossy dielectrics in the frequency domain is

$$\hat{\epsilon} = \epsilon + \frac{\sigma}{j\omega} \tag{2}$$

where ω is the radian frequency. The complex relative permittivity is determined using (2) as

$$\hat{\epsilon}_r = \frac{\hat{\epsilon}}{\epsilon_0} = \epsilon_r + \frac{\sigma}{j\omega\epsilon_0} \tag{3}.$$

If the material is a good conductor over all frequencies of interest, then the constitutive parameters satisfy the condition

$$\frac{\sigma}{\omega\epsilon} >> 1 \tag{4}.$$

Therefore, $\hat{\epsilon}_r$ can be approximated as

$$\hat{\epsilon}_r \approx \frac{\sigma}{j\omega\epsilon_0} \tag{5}.$$

Assuming parameters $\mu=\mu_0$ and $\epsilon=\epsilon_0$ and using the values of $\hat{\epsilon}_r$ and λ_0 at 10 GHz, the cell size is $\delta x = \delta y = \delta z = 1.582$ mm. If a SIBC is used, then the cell size need only be chosen to resolve the field in free space and (1) is modified to

$$\delta x_{SIBC} = \delta y_{SIBC} = \delta z_{SIBC} = \lambda_0/10 \tag{6}.$$

Again, using the value for λ_0 at 10 GHz, the cell size is $\delta x_{SIBC} = \delta y_{SIBC} = \delta z_{SIBC} = 3.0$ mm. Thus the cell size has been increased by the factor $\sqrt{|\hat{\epsilon}_r|} = 1.90$, and the computational storage requirements are reduced by the same factor. Therefore, the computational savings, denoted by S, is

$$S = \left[\sqrt{|\hat{\epsilon}_r|}\right]^d \tag{7}$$

where $\hat{\epsilon}_r$ is given by (5), (4) is satisfied for all frequencies of interest and d is the number of dimensions.

III. FDTD Constant Surface Impedance Implementation

To implement the constant SIBC in the FDTD method we consider the planar air-lossy dielectric interface as shown in Figure 1. The conducting material has permittivity ϵ, permeability μ and conductivity σ. We assume that the thickness of the material is large compared to the skin depth. We will also assume that the material is linear and isotropic and a basic familiarity with the Yee algorithm [1]. Figure 1 also shows the one-dimensional FDTD grid.

The first order (or Leontovich) impedance boundary condition relates tangential total field components and is given in the frequency domain as [6]

$$E_x(\omega) = Z_s(\omega) H_y(\omega) \tag{8}$$

where $Z_s(\omega)$ is the surface impedance of the conductor. The frequency domain surface impedance for good conductors is

$$Z_s(\omega) = (1+j)\sqrt{\frac{\omega\mu}{2\sigma}} = \sqrt{\frac{j\omega\mu}{\sigma}} \tag{9}.$$

Using (9), (8) can be rewritten as

$$E_x(\omega) = \left(R_s(\omega) + jX_s(\omega)\right) H_y(\omega) \tag{10}$$

where R_s is the surface resistance and X_s is the surface reactance. Consider rewriting (10) as

$$E_x(\omega) = \left(R_s(\omega) + j\omega L_s(\omega)\right) H_y(\omega) \tag{11}$$

with the resistance and inductance defined by

$$\begin{aligned} R_s(\omega) &= \sqrt{\frac{\omega\mu}{2\sigma}} \\ L_s(\omega) &= \sqrt{\frac{\mu}{2\sigma\omega}} \end{aligned} \tag{12}$$

To remove the frequency dependence of the surface resistance and inductance, these quantities are evaluated at a particular frequency and are subsequently treated as constants. Equation (11) then becomes

$$E_x(\omega) = \left(R_s + j\omega L_s\right) H_y(\omega) \qquad (13).$$

This is the required frequency domain constant surface impedance boundary condition. To incorporate this boundary condition into the FDTD algorithm, the time domain equivalent of (13) must be obtained. Performing an inverse Fourier transform operation on (13) results in

$$E_x(t) = R_s H_y(t) + L_s \frac{\partial}{\partial t} H_y(t) \qquad (14).$$

This equation defines the time domain FDTD constant surface impedance boundary condition.

To implement this constant surface impedance boundary condition, space and time are quantized by defining

$$\begin{aligned} z &\Rightarrow (k\delta z) \Rightarrow (k) \\ t &\Rightarrow (n\delta t) \Rightarrow (n) \end{aligned} \qquad (15).$$

The Faraday-Maxwell law is then used to obtain the H_y component in the free space cell next to the impedance boundary. Since the impedance boundary condition requires that the electric and magnetic fields are co-located in space and time, we assume that the magnetic field 1/2 cell in front of the impedance boundary and 1/2 time step previous is an adequate approximation. The Faraday-Maxwell law yields

$$-\left(\mu_0 \delta x \delta z\right)\left[\frac{\partial}{\partial (n\delta t)} HY^n(k+1/2)\right] = EX^n(k+1)\,\delta x - EX^n(k)\,\delta x \qquad (16).$$

Note the component $EX^n(k+1)$ of (16) is the electric field component at the impedance boundary. Quantizing space and time in (14) and using the result to eliminate $EX^n(k+1)$ in (16) gives

$$-\left(\mu_0 \delta z\right)\left[\frac{\partial}{\partial (n\delta t)} HY^n(k+1/2)\right] = R_s HY^n(k+1/2) + L_s\left[\frac{\partial}{\partial (n\delta t)} HY^n(k+1/2)\right] - EX^n(k) \qquad (17).$$

Notice that the $HY^n(k+1/2)$ term in (17) is time indexed at time step n. This term is approximated as

$$HY^{n}(k+1/2) \approx \frac{1}{2}\left[HY^{n+1/2}(k+1/2) + HY^{n-1/2}(k+1/2)\right] \qquad (18).$$

Using (18), and approximating the time derivatives on the magnetic fields in (17) as finite differences gives

$$-\left(\mu_0\delta z + L_s\right)\left(HY^{n+1/2}(k+1/2) - HY^{n-1/2}(k+1/2)\right) = \frac{R_s\delta t}{2}\left(HY^{n+1/2}(k+1/2) - HY^{n-1/2}(k+1/2)\right) - \delta t\, EX^{n}(k) \qquad (19).$$

Solving for $HY^{n+1/2}(k+1/2)$ in (19) yields

$$HY^{n+1/2}(k+1/2) = \left[\frac{\mu_0\delta z + L_s - R_s\delta t/2}{\mu_0\delta z + L_s + R_s\delta t/2}\right] HY^{n-1/2}(k+1/2) - \frac{\delta t}{\mu_0\delta z + L_s + R_s\delta t/2}\, EX^{n}(k) \qquad (20).$$

This equation implements the constant surface impedance boundary condition in the FDTD method.

IV. FDTD Dispersive Surface Impedance Implementation

To derive a similar relation to (20) valid over a wide frequency band, we begin with the same set of underlying assumptions as for the constant surface impedance. The primary exception is that the surface impedance will vary with frequency and will not be approximated by its value at a particular frequency. All frequency domain information is inversed Fourier transformed to equivalent time domain form. The SIBC is then implemented in the FDTD method with the required convolution using a recursive updating technique.

The standard first order impedance boundary condition remains unchanged and is given by (8). In a similar fashion as Tesche [9], (8) is rewritten as

$$E_x(\omega) = j\omega\left[\frac{Z_s(\omega)}{j\omega}\right] H_y(\omega) \qquad (21).$$

Defining

$$Z_s'(\omega) = \frac{Z_s(\omega)}{j\omega} \tag{22}$$

and substituting (9) into (22) gives

$$Z_s'(\omega) = \sqrt{\frac{\mu}{j\omega\sigma}} \tag{23}.$$

Substituting (23) into (21), a modified surface impedance boundary condition is obtained as

$$E_x(\omega) = Z_s'(\omega)\,[j\omega H_y(\omega)] \tag{24}.$$

The time domain equivalent of (24) is obtained via an inverse Fourier transform operation as

$$E_x(t) = Z_s'(t) * \left[\frac{\partial}{\partial t} H_y(t)\right] \tag{25}$$

where the asterisk denotes convolution,

$$\begin{aligned} E_x(t) &= \mathcal{F}^{-1}[E_x(\omega)] \\ H_y(t) &= \mathcal{F}^{-1}[H_y(\omega)] \\ Z_s'(t) &= \mathcal{F}^{-1}[Z_s'(\omega)] \end{aligned} \tag{26}$$

and the $\mathcal{F}^{-1}$ denotes the inverse Fourier transform operation. Note in (25) that as $\sigma \rightarrow \infty$, the boundary condition becomes $E_x(t)=0.0$, which is required for a perfect conductor. To determine $Z_s'(t)$, the Laplace transform variable $s=j\omega$ is used in (23) to obtain

$$Z_s'(s) = \sqrt{\frac{\mu}{\sigma}}\,\frac{1}{\sqrt{s}} \tag{27}.$$

Using the Laplace transform pair [11]

$$\frac{1}{\sqrt{\pi t}} = \mathcal{L}^{-1}\left[\frac{1}{\sqrt{s}}\right] \tag{28}$$

where the $\mathcal{L}^{-1}$ denotes the inverse Laplace transform operation; and $Z_s'(t)$ is then determined to be

$$Z_s'(t) = \mathcal{F}^{-1}[Z_s'(\omega)] = \begin{cases} \sqrt{\dfrac{\mu}{\pi\sigma t}}, & t > 0 \\ 0, & t < 0 \end{cases} \tag{29}.$$

This is the required time domain surface impedance function. Substituting (29) into (25) and discretizing space and time according to (15) gives

$$EX^n(k+1) = \sqrt{\frac{\mu}{\pi\sigma(n\delta t)}} * \left[\frac{\partial}{\partial(n\delta t)} HY^n(k+1/2)\right] \tag{30}.$$

Substituting (30) into (16) yields

$$-\mu_0\delta z\left[\frac{\partial}{\partial(n\delta t)} HY^n(k+1/2)\right] = \sqrt{\frac{\mu}{\pi\sigma(n\delta t)}} * \left[\frac{\partial}{\partial(n\delta t)} HY^n(k+1/2)\right] - EX^n(k) \tag{31}.$$

The convolution in (31) is expressed as a summation to obtain

$$-\mu_0\delta z\left[\frac{\partial}{\partial(n\delta t)} HY^n(k+1/2)\right] = \sqrt{\frac{\mu\delta t}{\pi\sigma}} \sum_{m=0}^{n-1}\left[\frac{\partial}{\partial((n-m)\,\delta t)} HY^{n-m}(k+1/2)\right] Z_0(m) - EX^n(k) \tag{32}$$

where $Z_0(m)$ is the discrete impulse response. The discrete impulse response is obtained by assuming the fields are piecewise constant in time as

$$Z_0(m) = \int_{m-1/2}^{m+1/2} \frac{1}{\sqrt{\alpha}}\, d\alpha \tag{33}$$

If m=0, the lower limit in (33) is 0. Approximating the time derivatives on the magnetic fields in (32) as finite differences results in

$$\left[HY^{n+1/2}(k+1/2) - HY^{n-1/2}(k+1/2)\right] = -Z_1 \sum_{m=0}^{n-1} \left[HY^{n-m+1/2}(k+1/2) - HY^{n-m-1/2}(k+1/2)\right] Z_0(m) + \frac{\delta t}{\mu_0 \delta z} EX^n(k) \tag{34}$$

where

$$Z_1 = \frac{1}{\mu_0 \delta z} \sqrt{\frac{\mu \delta t}{\pi \sigma}} \tag{35}.$$

Equation (34) is suitable for computer implementation and includes the full convolution with all past field components. This full convolution would be impractical for large three dimensional problems; thus it is desirable to obtain a more efficient implementation. The development of a recursive implementation is the subject of the following section.

V. Recursive Implementation

Recently, Luebbers et. al. [3] extended the FDTD technique to dispersive dielectric materials using a time domain susceptibility function for polar dielectrics. In that paper, the time domain susceptibility function was a decaying exponential which permits the convolution summation to be recursively updated, thus avoiding the need for the complete time history of field components. Upon further examination of (34), it is clear that if $Z_0(m)$ can be approximated by a series of exponentials, then the SIBC can be efficiently evaluated using recursion. Figure 2 shows $Z_0(m)$ versus m, and it is clear that it can be approximated by a series of exponentials. $Z_0(m)$ is approximated as

$$Z_0(m) \approx \sum_{i=1}^{N} a_i e^{\alpha_i m} \tag{36}$$

where N is the number of terms in the approximation. One of the most accurate methods for obtaining an exponential approximation to an exact function or to a data set is Prony's method [10]. Figure 2 also shows the Prony approximation to $Z_0(m)$ with N=10 and it is clear that N=10 provides an adequate approximation. Thus, using (36) with N=10 in (34) gives

$$HY^{n+1/2}(k+1/2) = HY^{n-1/2}(k+1/2) - \frac{Z_1}{1+Z_1Z_0(0)} \sum_{i=1}^{10}\sum_{m=1}^{n-1}\left[HY^{n-m+1/2}(k+1/2) - HY^{n-m-1/2}(k+1/2)\right]\cdot a_i e^{\alpha_i m} + \frac{\delta t}{\mu_0 \delta z (1+Z_1Z_0(0))} EX^n(k) \tag{37}$$

where

$$Z_0(0) = \sum_{i=1}^{10} a_i \tag{38}.$$

The convolution can now be recursively updated (see Appendix) to give

$$HY^{n+1/2}(k+1/2) = HY^{n-1/2}(k+1/2) - \frac{Z_1}{1+Z_1Z_0(0)} \sum_{i=1}^{10} \psi_i^n(k+1/2) + \frac{\delta t}{\mu_0 \delta z (1+Z_1Z_0(0))} EX^n(k) \tag{39}$$

Note that only one past value of magnetic field is required to update the convolution summation.

VI. One Dimensional Demonstration

To demonstrate the constant and recursive FDTD SIBC, (20) and (39) were implemented in a one dimensional total field FDTD code for the geometry shown in Figure 1. The problem space size is 301 cells, the impedance boundary is located at cell 300, and the electric field is sampled at cell 299. The maximum frequency of interest for each problem was 10 GHz. The incident electric field is a Gaussian pulse with maximum amplitude of 1000 V/m and has a total temporal width of 256 time steps. The frequency response of the incident pulse contains significant information to 12 GHz. Two computations were made with σ=2.0 S/m and σ=20.0 S/m. The loss tangents at 10 GHz are 3.599, 35.99, respectively. The permittivity and permeability for the lossy dielectric were those of free space. The cell size and time step were 750 μm and 2.5 psec, respectively. A tie point of 5.0 GHz was chosen for the FDTD constant SIBC. For each FDTD computation, a reflection coefficient versus frequency was obtained by first dividing the Fourier transform of the scattered field by the transform of the incident field at cell 299. The incident field was obtained by running the FDTD code with free space only and recording the electric field at cell 299. The scattered field is then obtained by subtracting the

time domain incident field from time domain total field. The results are compared with the analytic surface impedance reflection coefficient computed from

$$|R| = \frac{|Z_s(\omega) - \eta_0|}{|Z_s(\omega) + \eta_0|} \tag{40}$$

where $Z_s(\omega)$ is given by (9) and η_0 is the free space wave impedance. The phase of the FDTD reflection coefficient was corrected to account for the round trip phase shift of one cell since the FDTD reflection coefficient is computed from electric fields recorded one cell in front of the impedance boundary.

The high conductivity surface impedance of (9) is an approximation to the general surface impedance for lossy dielectrics given by

$$Z_s(\omega) = \sqrt{\frac{j\omega\mu}{\sigma + j\omega\epsilon}} \tag{41}.$$

The advantage of using (9) over (41) for the FDTD SIBC implementation is that the resulting time domain impulse response is independent of the conductivity. The exponential approximation needs to be performed only once and not each time the conductivity is changed.

Figures 3-4 show the FDTD constant and recursive SIBC reflection coefficient magnitude and phase results versus the analytic SIBC results for σ=2.0 S/m. Notice the agreement between the curves is good, and the maximum error is about 0.02 at 10 GHz in Figure 3.

Figures 5-6 show the FDTD constant and recursive SIBC reflection coefficient magnitude and phase results versus the analytic SIBC results for σ=20.0 S/m. Notice the agreement between the curves is excellent.

Since the FDTD SIBC implementation is an approximation to an analytic SIBC, some amount of divergence between the SIBC curves and the analytic SIBC solution is to be expected with increasing frequency. As frequency increases, the effective number of cells per wavelength decreases and the FDTD SIBC becomes a rougher approximation to the analytic SIBC. To observe this error trend, the same one-dimensional test problems as above (using the dispersive SIBC only) were reevaluated with larger cell sizes equal to twice and four times the original cell size. This is equivalent to having 20 and 10 cells/λ_0 in the free space region, respectively. Figures 7 and 8 show the FDTD dispersive SIBC

reflection coefficient magnitude and phase results versus the analytic SIBC for σ=2.0 S/m using the original cell size and the larger cell sizes. Notice that for each increase in cell size, the agreement between the SIBC curve and the exact solution is reduced by a factor of two. This indicates that the error in the SIBC implementation is $O(\delta z)$ over the range of cell sizes examined here. The constant SIBC exhibited similar agreement reductions at the 5 GHz tie point for larger cell sizes.

VIII. Two Dimensional Demonstration

As a practical application of the FDTD dispersive SIBC, frequency domain scattering width was computed from an infinite square cylinder for two scattering angles, ϕ=0.0 and ϕ=30.0 degrees using a full two dimensional TM scattered field code. The cylinder was 0.99 cm square and had parameters $\epsilon=\epsilon_0$, $\mu=\mu_0$, and σ=20.0 S/m. To illustrate the applicability of the SIBC, the cylinder was modeled in two ways. The first was a normal FDTD computation with a grid size of 10 cells/λ (at 10 GHz) inside the conducting cylinder and the second was a SIBC computation with a grid size of 10 cells/λ in free space (at 10 GHz). Figure 7 shows the two dimensional field components and the cylinder dimensions (in cells) for the FDTD and SIBC computations. For the FDTD computation, the cylinder was modeled using 198 cells in the x and y directions, the cell size was 500 μm, and the time step was 1.18 ps. For the SIBC computation, the cylinder was modeled using 32 cells in the x and y directions, the cell size was 0.003 m and the time step was 7.07 ps. For both computations, a 100 cell border between the cylinder and the absorbing boundary was chosen, the total number of time steps was 1024, and an incident Gaussian pulse with total pulse width of 64 time steps was chosen. The near zone fields were transformed to far zone fields by a two-dimensional near zone to far zone transformation [12].

Figure 10 shows the scattering width magnitude versus frequency for a scattering angle of ϕ=0.0 degrees using the FDTD computation and the SIBC computation. Notice the good agreement over the entire frequency bandwidth for the dispersive SIBC.

Figure 11 shows the scattering width magnitude versus frequency for a scattering angle of ϕ=30.0 degrees using the FDTD computation and the SIBC computation. Notice again the good agreement over the entire frequency bandwidth for the dispersive SIBC.

IX. Summary

One dimensional FDTD implementations of constant and dispersive surface impedance boundary conditions have been presented. The corresponding time domain impedance boundary conditions have been derived and their validity demonstrated by one-dimensional computation of the reflection coefficient at an

air-lossy dielectric interface at a single frequency and over a wide frequency bandwidth. The applicability of the SIBC to two-dimensional scattering problems was demonstrated by scattering width computation from an infinite square cylinder. For both the one and two dimensional cases, the dispersive FDTD results were shown to be in good agreement with exact results over the entire bandwidth. Considerable computational savings were illustrated and a recursive updating scheme was implemented which permits efficient application of a dispersive surface impedance boundary condition to practical scattering problems.

Future extensions of this surface impedance concept currently under investigation are implementation in three dimensions, inclusion of surface curvature, dispersive dielectric and magnetic materials and thin material layers.

X. Acknowledgements

The authors wish to thank the reviewers for helpful comments and suggestions.

Appendix

The purpose of this Appendix is to show how the discrete convolution of the SIBC in (37) can be done recursively. The convolution in (37) is

$$\sum_{i=1}^{10}\sum_{m=1}^{n-1}\left[HY^{n-m+1/2}(k+1/2) - HY^{n-m-1/2}(k+1/2)\right] a_i e^{\alpha_i m} \qquad (42)$$

Consider n=2, and (42) becomes

$$\sum_{i=1}^{10}\left(HY^{3/2}(k+1/2) - HY^{1/2}(k+1/2)\right) a_i e^{\alpha_i} \qquad (43).$$

Now define

$$\psi_i^2(k+1/2) = \left(HY^{3/2}(k+1/2) - HY^{1/2}(k+1/2)\right) a_i e^{\alpha_i} \qquad (44).$$

Next for n=3, (42) becomes

$$\sum_{i=1}^{10}\sum_{m=1}^{2}\left(HY^{7/2-m}(k+1/2) - HY^{5/2-m}(k+1/2)\right) a_i e^{\alpha_i m} \qquad (45).$$

Expanding (45) gives

$$\begin{aligned}&\sum_{i=1}^{10}\left(HY^{5/2}(k+1/2) - HY^{3/2}(k+1/2)\right) a_i e^{\alpha_i} + \\ &\quad \left(HY^{3/2}(k+1/2) - HY^{1/2}(k+1/2)\right) a_i e^{2\alpha_i}\end{aligned} \qquad (46).$$

Substituting (44) into (46) we obtain

$$\sum_{i=1}^{10}\left[\left(HY^{5/2}(k+1/2) - HY^{3/2}(k+1/2)\right) a_i e^{\alpha_i} + e^{\alpha_i}\psi_i^2(k+1/2)\right] \qquad (47).$$

Equation (47) can be generalized for any time step n as

$$\sum_{i=1}^{10}\left[\left(HY^{n-1/2}(k+1/2) - HY^{n-3/2}(k+1/2)\right) a_i e^{\alpha_i} + e^{\alpha_i}\psi_i^{n-1}(k+1/2)\right] \qquad (48).$$

with

$$\psi_i^n(k+1/2) = \left(HY^{n-1/2}(k+1/2) - HY^{n-3/2}(k+1/2)\right)a_i e^{\alpha_i} + e^{\alpha_i}\psi^{n-1}(k+1/2) \tag{49}$$

and

$$\psi_i^1(k+1/2) = \psi_i^0(k+1/2) = 0.0 \tag{50}$$

REFERENCES

[1] K. S. Yee, "Numerical solution of initial boundary value problems involving Maxwell's equations in isotropic media," IEEE Trans. Antennas Propagat., vol. AP-14, pp. 302-307, May 1966.

[2] A. Taflove and K. Umashankar, "The Finite-Difference Time Domain method for numerical modeling of electromagnetic wave interactions with arbitrary structures," in PIER2: Progress in Electromagnetics Research, M. A. Morgan (editor), New York: Elsevier, pp. 287-373, 1990.

[3] R. J. Luebbers et al, "A frequency dependent Finite Difference Time Domain formulation for dispersive materials,"IEEE Trans. Electromagn. Compat., vol. EMC-32, pp. 222-227, August 1990.

[4] F. P. Hunsberger, R. J. Luebbers and K. S. Kunz, "Application of the Finite-Difference Time-Domain method to electromagnetic scattering from 3-D chiral objects," Proc. IEEE AP-S Int. Symp., Dallas, TX, May 1990, vol. 1, pp. 38-41.

[5] R. J. Luebbers et al, "A frequency dependent Finite Difference Time Domain formulation for transient propagation in plasmas," IEEE Trans. Antennas Propagat., vol. AP-39, pp. 29-34, Jan. 1991.

[6] M. A. Leontovich, "On the approximate boundary conditions for electromagnetic fields on the surface of well conducting bodies," in Investigations of propagation of radio waves, B. A. Vvedensky (editor), Academy of Sciences USSR, Moscow, pp. 5-20, 1948.

[7] T. B. A. Senior, "Impedance boundary conditions for imperfectly conducting surfaces," Appl. Sci. Res. B, vol. 8, pp. 418-436, 1960.

[8] J. G. Maloney and G. S. Smith, "Implementation of surface impedance concepts in the Finite Difference Time Domain (FD-TD) technique," Proc. 1990 IEEE AP-S Int. Symp., Dallas, TX, May 1990, vol. 4, pp. 1628-1631.

[9] Frederick M. Tesche, "On the inclusion of loss in time-domain solutions of electromagnetic interaction problems," IEEE Trans. Electromagn. Compat., vol. EMC-32, pp. 1-4, Feb. 1990.

[10] F. B. Hildebrand, Introduction to Numerical Analysis, New York: McGraw-Hill, 1956, pp. 378-382.

[11] Ruel V. Churchill, Operational Mathematics, New York: McGraw-Hill, 1972, p. 459.

[12] R. J. Luebbers, D. A. Ryan, J. H. Beggs and K. S. Kunz, "A Two-Dimensional Time Domain Near Zone to Far Zone Transformation," submitted to IEEE Trans. Antennas Propagat. for publication, May 1991.

FIGURE TITLES

1. Problem geometry showing one-dimensional FDTD grid and planar free space-conductor interface.

2. FDTD dispersive SIBC discrete impulse response $Z_0(m)$ versus m and Prony approximation using 10 terms.

3. Reflection coefficient magnitude versus frequency for normal incidence plane wave calculated for σ=2.0 S/m using FDTD constant and dispersive SIBC and analytic solution.

4. Reflection coefficient phase versus frequency for normal incidence plane wave calculated for σ=2.0 S/m using FDTD constant and dispersive SIBC and analytic solution.

5. Reflection coefficient magnitude versus frequency for normal incidence plane wave calculated for σ=20.0 S/m using FDTD constant and dispersive SIBC and analytic solution.

6. Reflection coefficient phase versus frequency for normal incidence plane wave calculated for σ=20.0 S/m using FDTD constant and dispersive SIBC and analytic solution.

7. Reflection coefficient magnitude versus frequency for normal incidence plane wave calculated for σ=2.0 S/m using FDTD dispersive SIBC with original and larger cell size and analytic solution.

8. Reflection coefficient phase versus frequency for normal incidence plane wave calculated for σ=2.0 S/m using FDTD dispersive SIBC with original and larger cell size and analytic solution.

9. Two dimensional geometry for scattering width computations from an infinite square cylinder with σ=20.0 S/m using normal FDTD and FDTD dispersive SIBC.

10. Scattering width magnitude versus frequency at scattering angle ϕ=0.0 degrees from an infinite square cylinder with σ=20.0 S/m using normal FDTD and FDTD dispersive SIBC.

11. Scattering width magnitude versus frequency at scattering angle ϕ=30.0 degrees from an infinite square cylinder with σ=20.0 S/m using normal FDTD and FDTD dispersive SIBC.

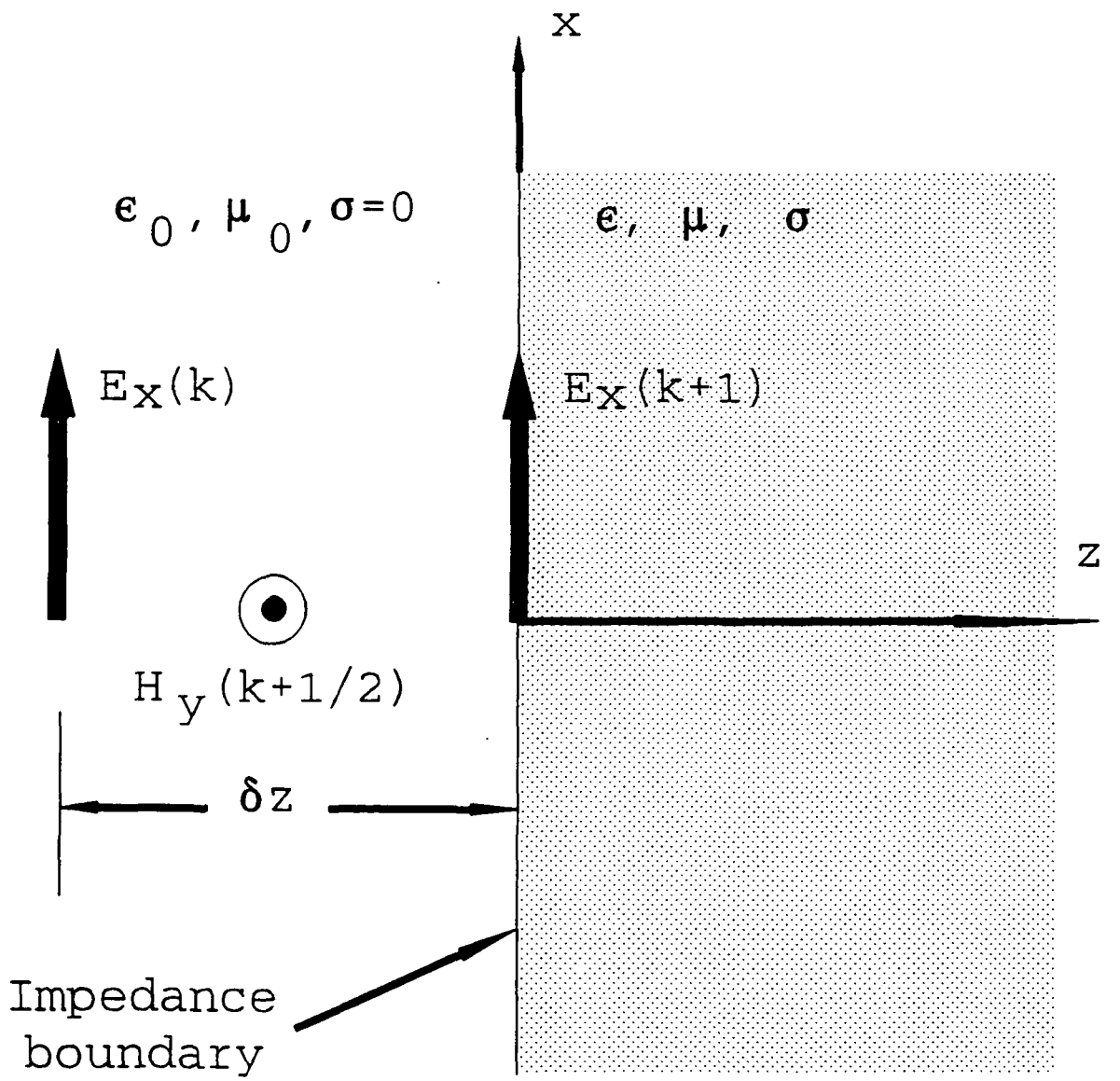
x
$\epsilon_0, \mu_0, \sigma=0$
ϵ, μ, σ
$E_x(k)$
$E_x(k+1)$
z
$H_y(k+1/2)$
δz
Impedance
boundary

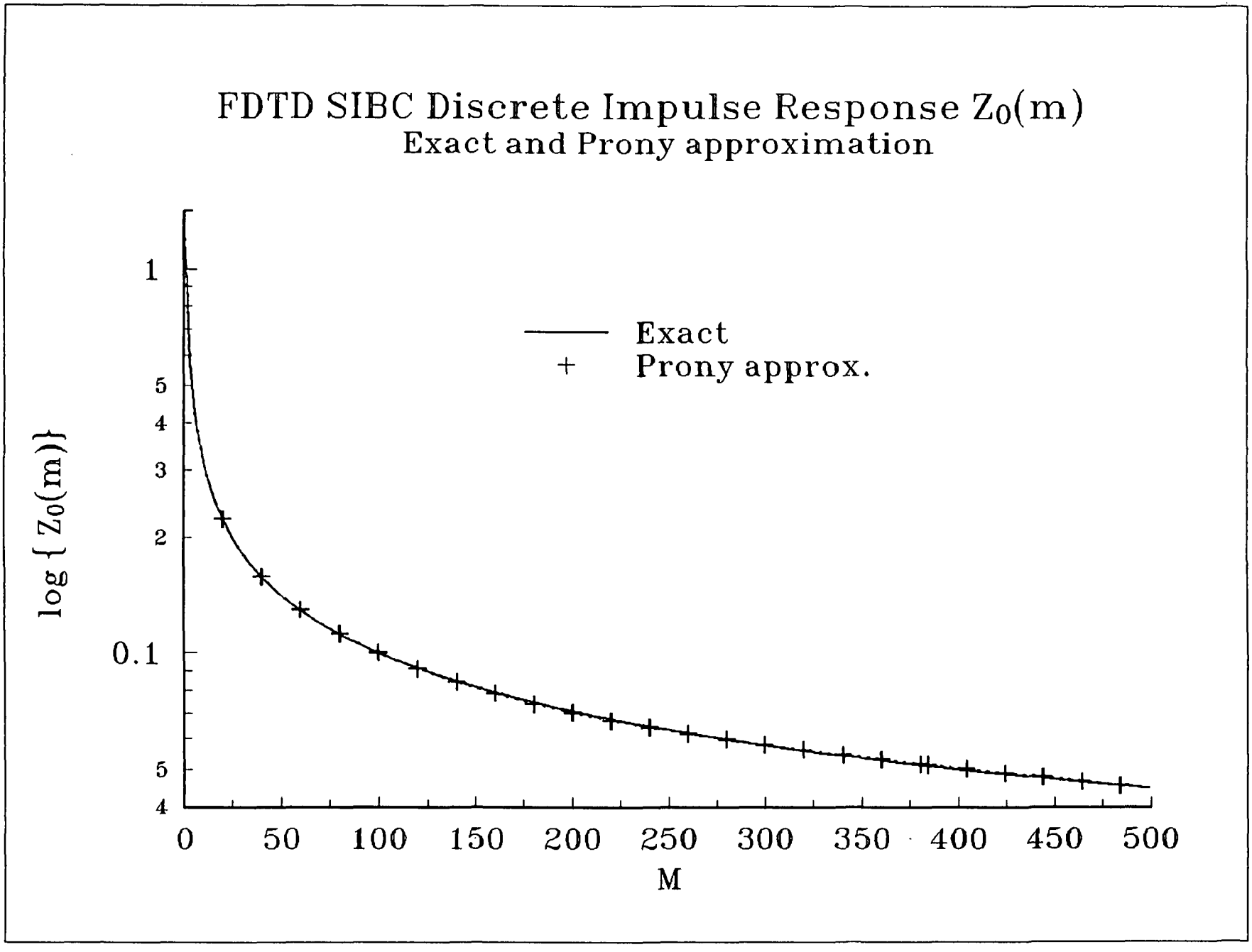
FDTD SIBC Discrete Impulse Response $Z_0(m)$
Exact and Prony approximation
Exact
Prony approx.
log { $Z_0(m)$ }
1
5
4
3
2
0.1
5
4
0
50
100
150
200
250
300
350
400
450
500
M

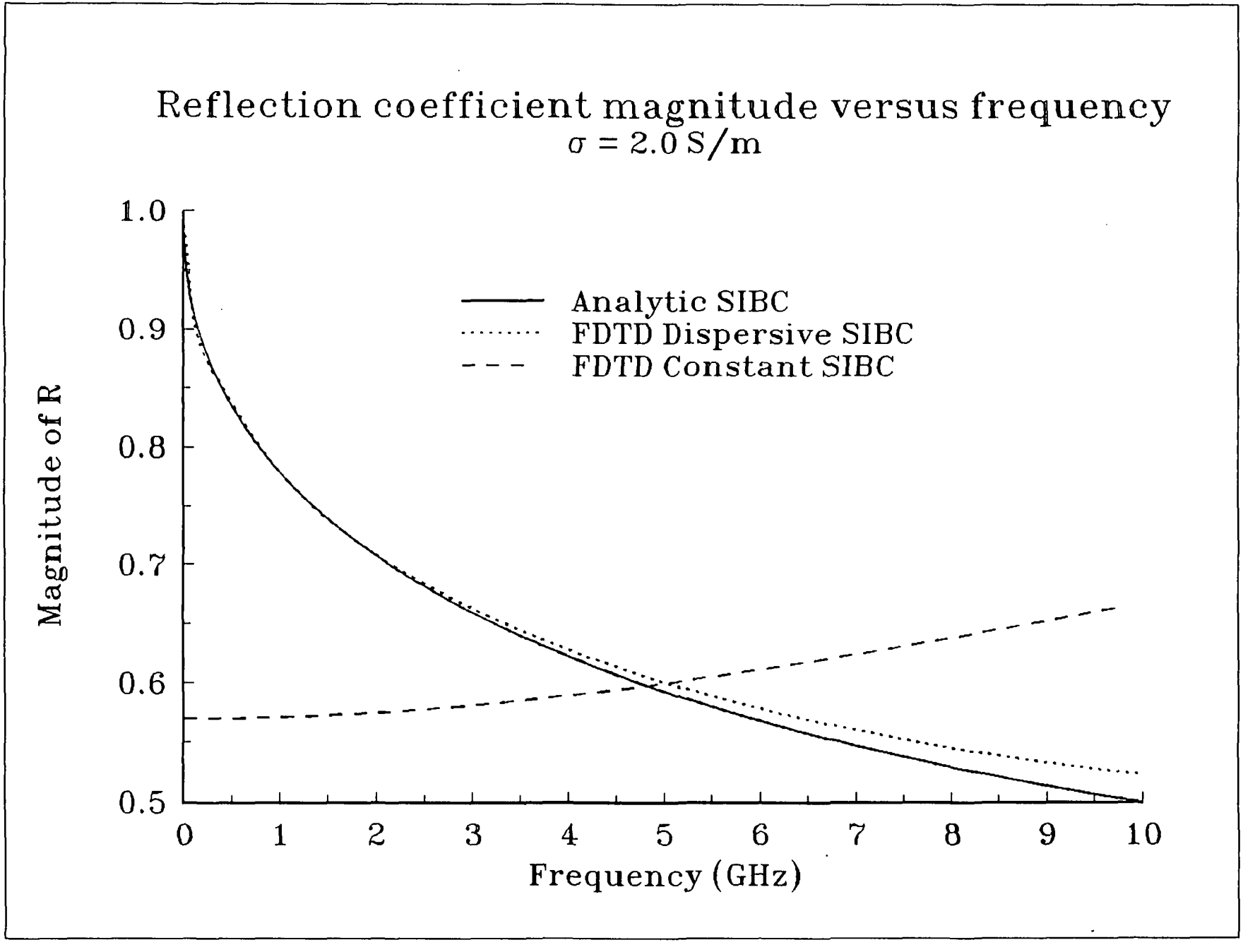
Reflection coefficient magnitude versus frequency
σ = 2.0 S/m
Analytic SIBC
FDTD Dispersive SIBC
FDTD Constant SIBC
Magnitude of R
1.0
0.9
0.8
0.7
0.6
0.5
0
1
2
3
4
5
6
7
8
9
10
Frequency (GHz)

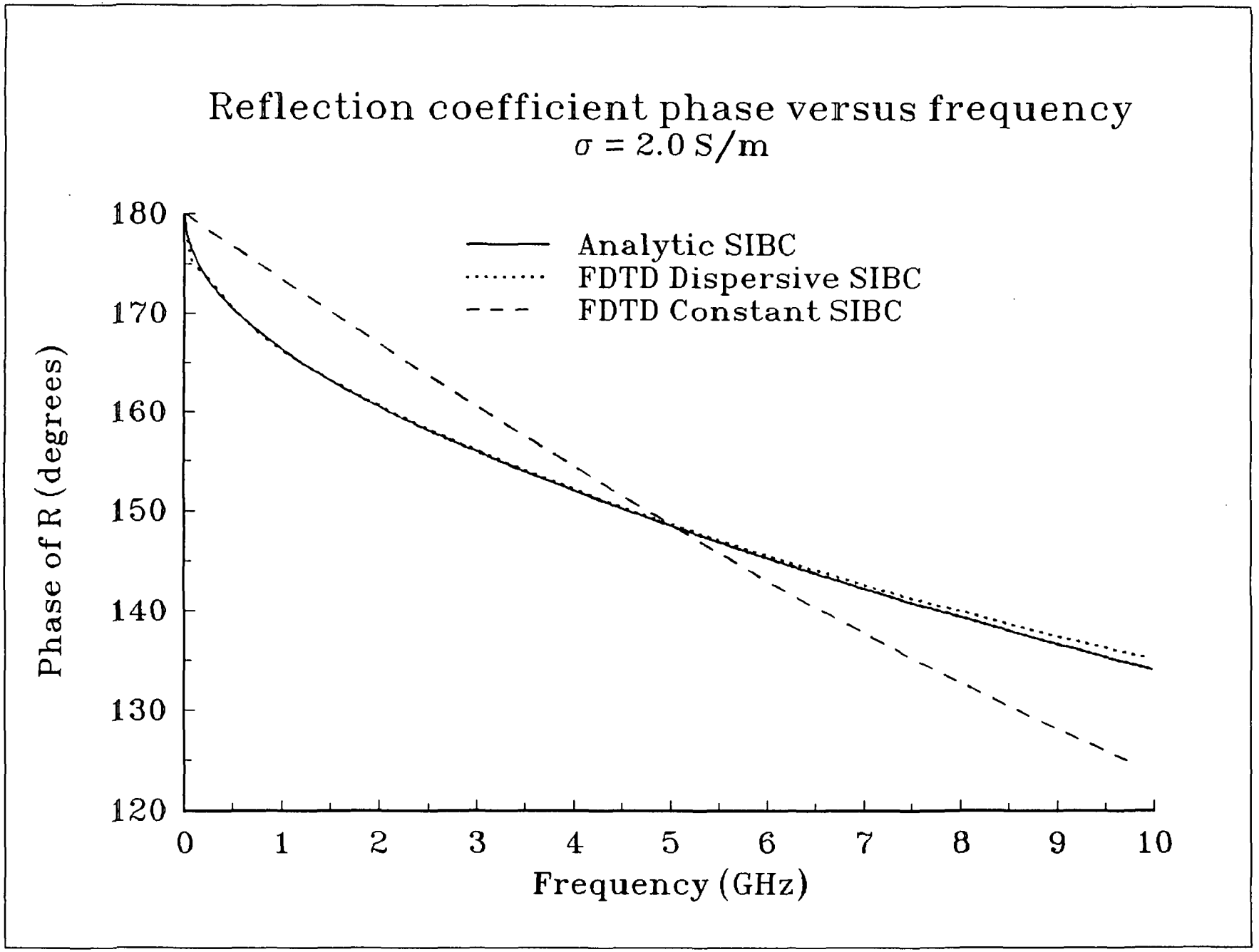
Reflection coefficient phase versus frequency
σ = 2.0 S/m
Analytic SIBC
FDTD Dispersive SIBC
FDTD Constant SIBC
Phase of R (degrees)
180
170
160
150
140
130
120
0
1
2
3
4
5
6
7
8
9
10
Frequency (GHz)

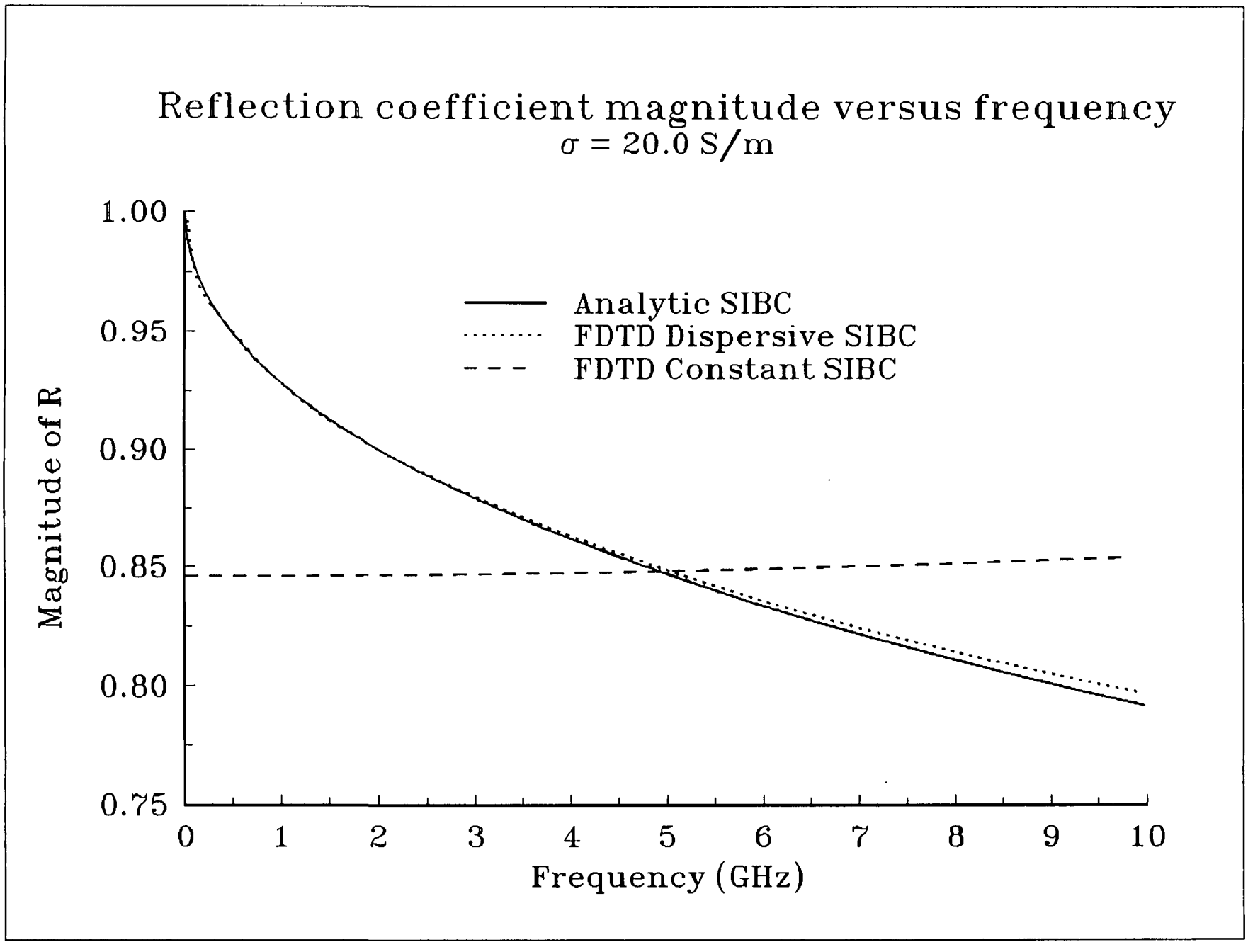
Reflection coefficient magnitude versus frequency
σ = 20.0 S/m
Analytic SIBC
FDTD Dispersive SIBC
FDTD Constant SIBC
Magnitude of R
1.00
0.95
0.90
0.85
0.80
0.75
0
1
2
3
4
5
6
7
8
9
10
Frequency (GHz)

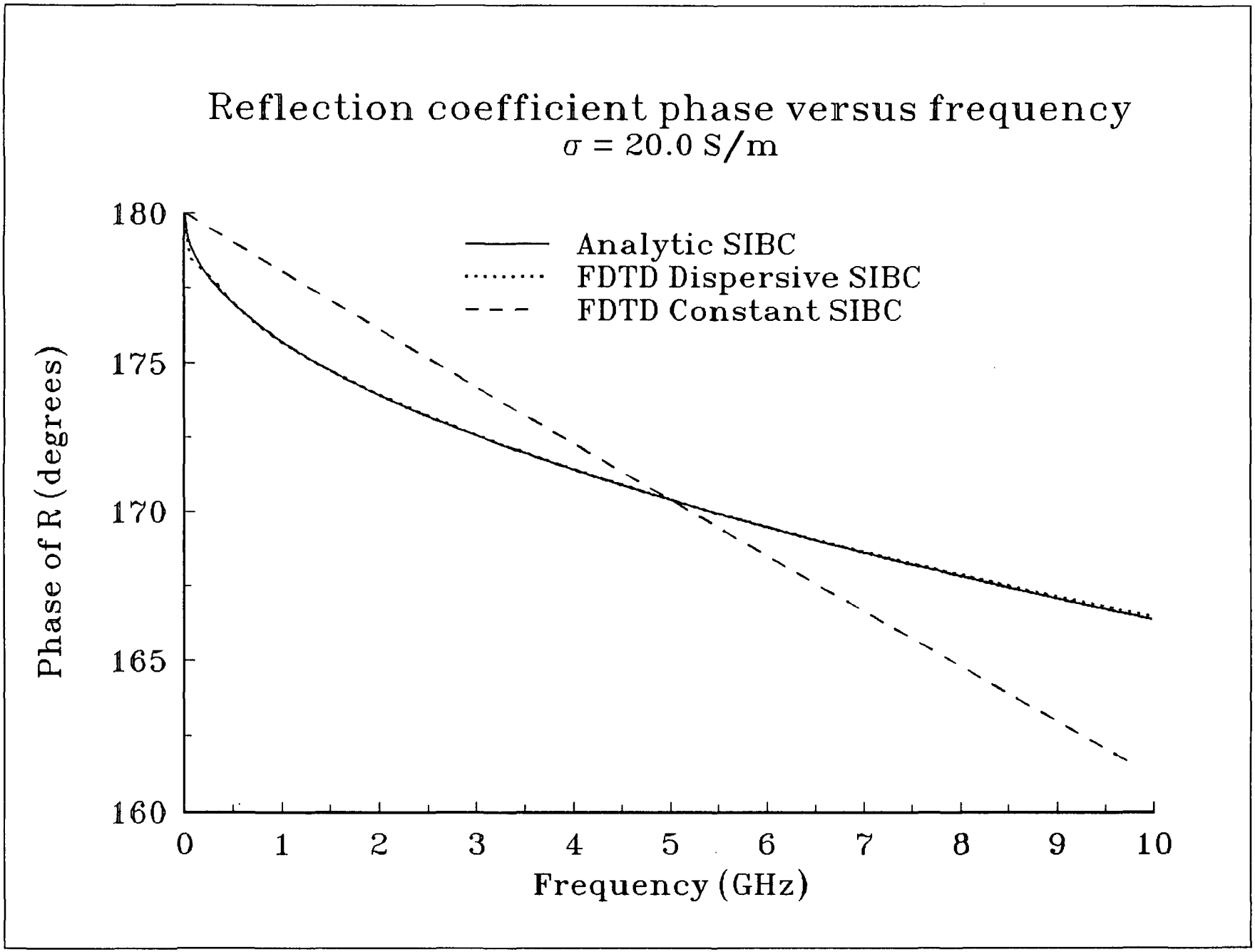
Reflection coefficient phase versus frequency
σ = 20.0 S/m
Analytic SIBC
FDTD Dispersive SIBC
FDTD Constant SIBC
Phase of R (degrees)
180
175
170
165
160
0
1
2
3
4
5
6
7
8
9
10
Frequency (GHz)

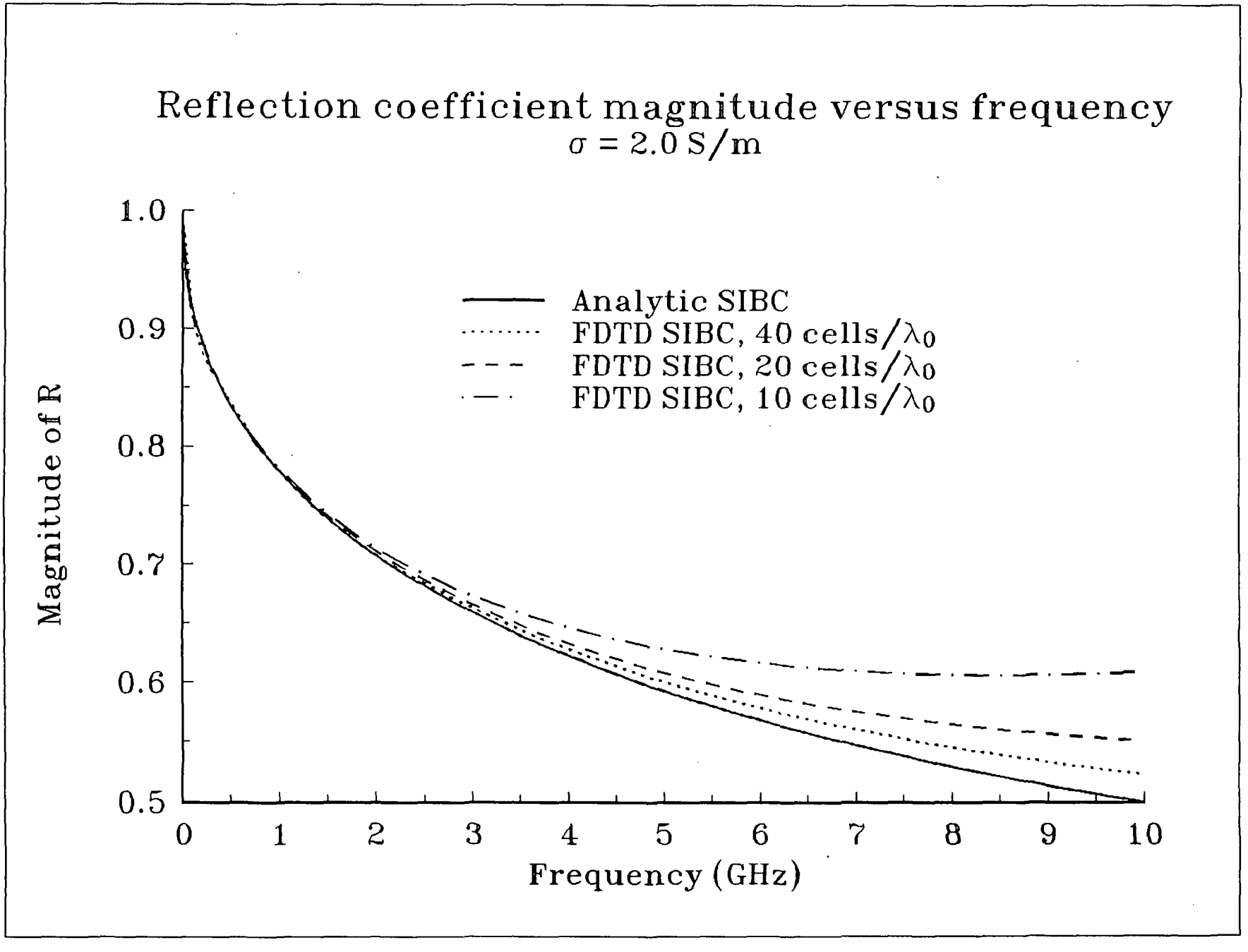
Reflection coefficient magnitude versus frequency
σ = 2.0 S/m
Magnitude of R
1.0
0.9
0.8
0.7
0.6
0.5
0
1
2
3
4
5
6
7
8
9
10
Frequency (GHz)
Analytic SIBC
FDTD SIBC, 40 cells/λ0
FDTD SIBC, 20 cells/λ0
FDTD SIBC, 10 cells/λ0

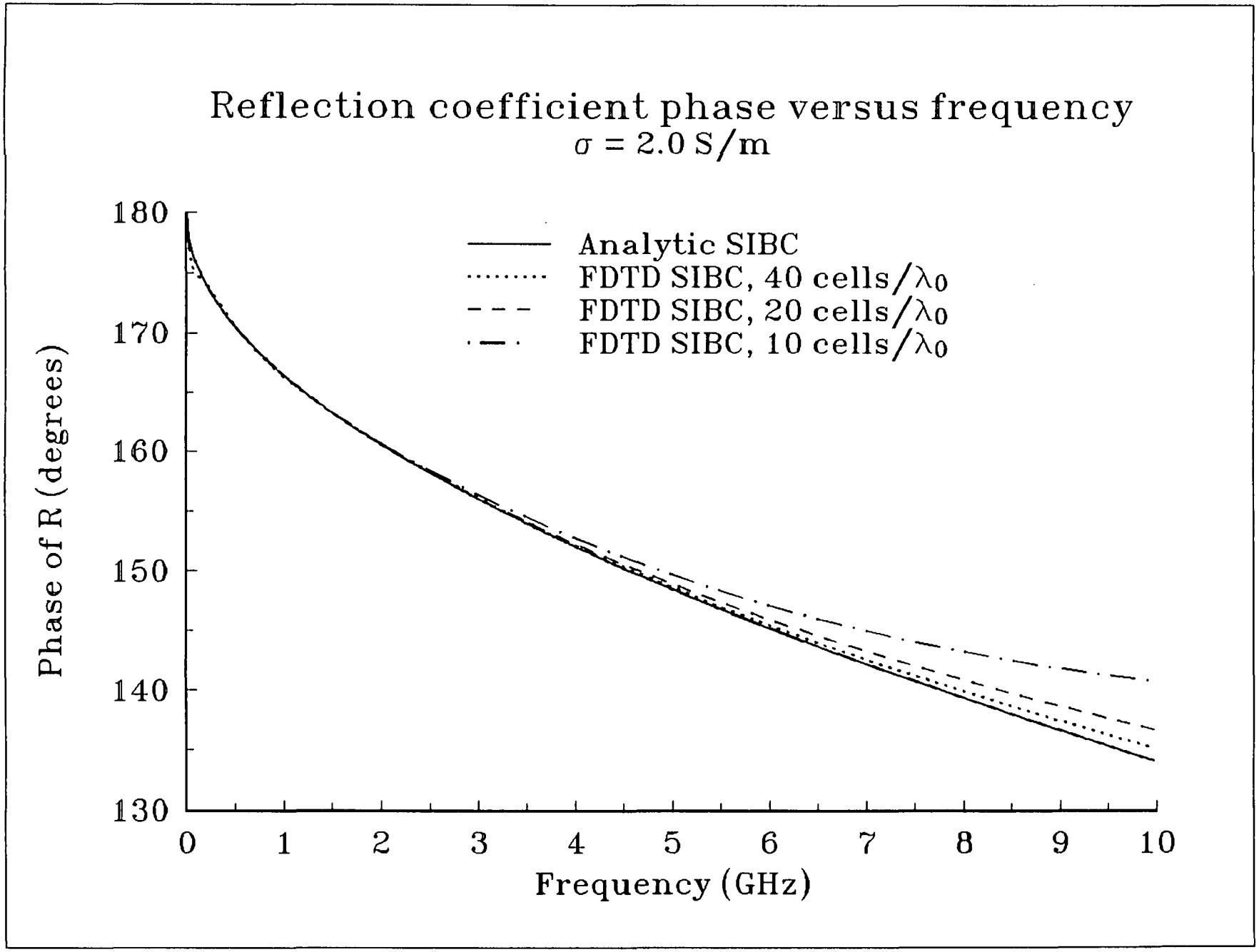
Reflection coefficient phase versus frequency
σ = 2.0 S/m
Analytic SIBC
FDTD SIBC, 40 cells/λ0
FDTD SIBC, 20 cells/λ0
FDTD SIBC, 10 cells/λ0
Phase of R (degrees)
180
170
160
150
140
130
0
1
2
3
4
5
6
7
8
9
10
Frequency (GHz)

2D TM FDTD grid

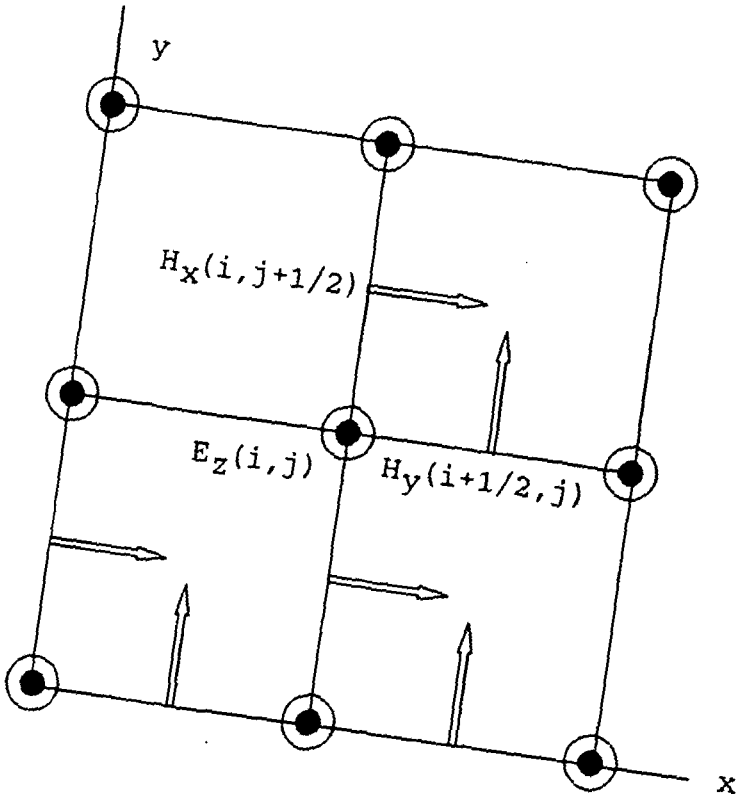

Normal FDTD computation

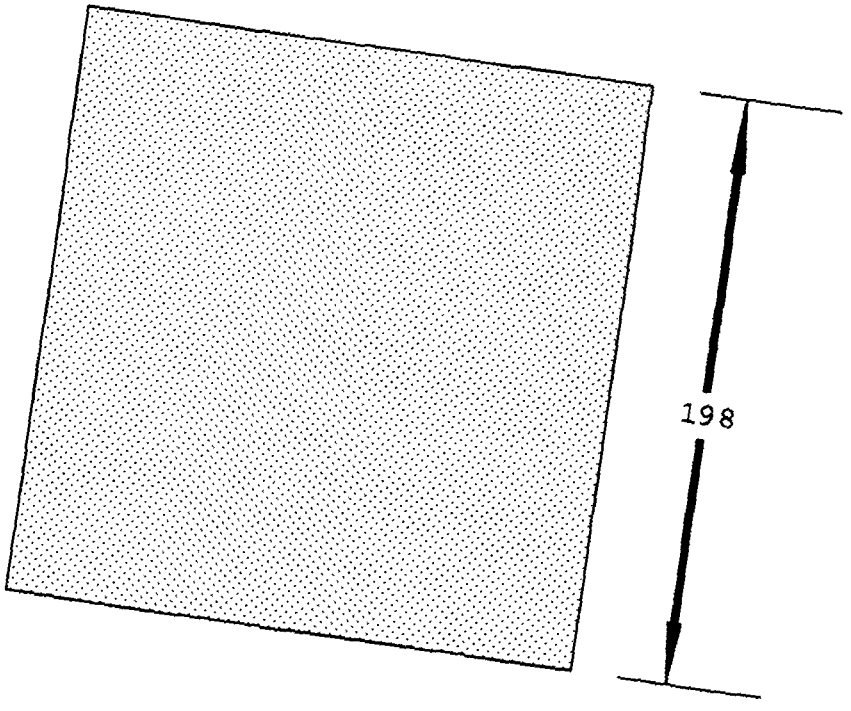

FDTD SIBC computation

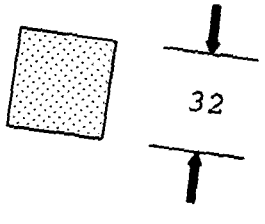

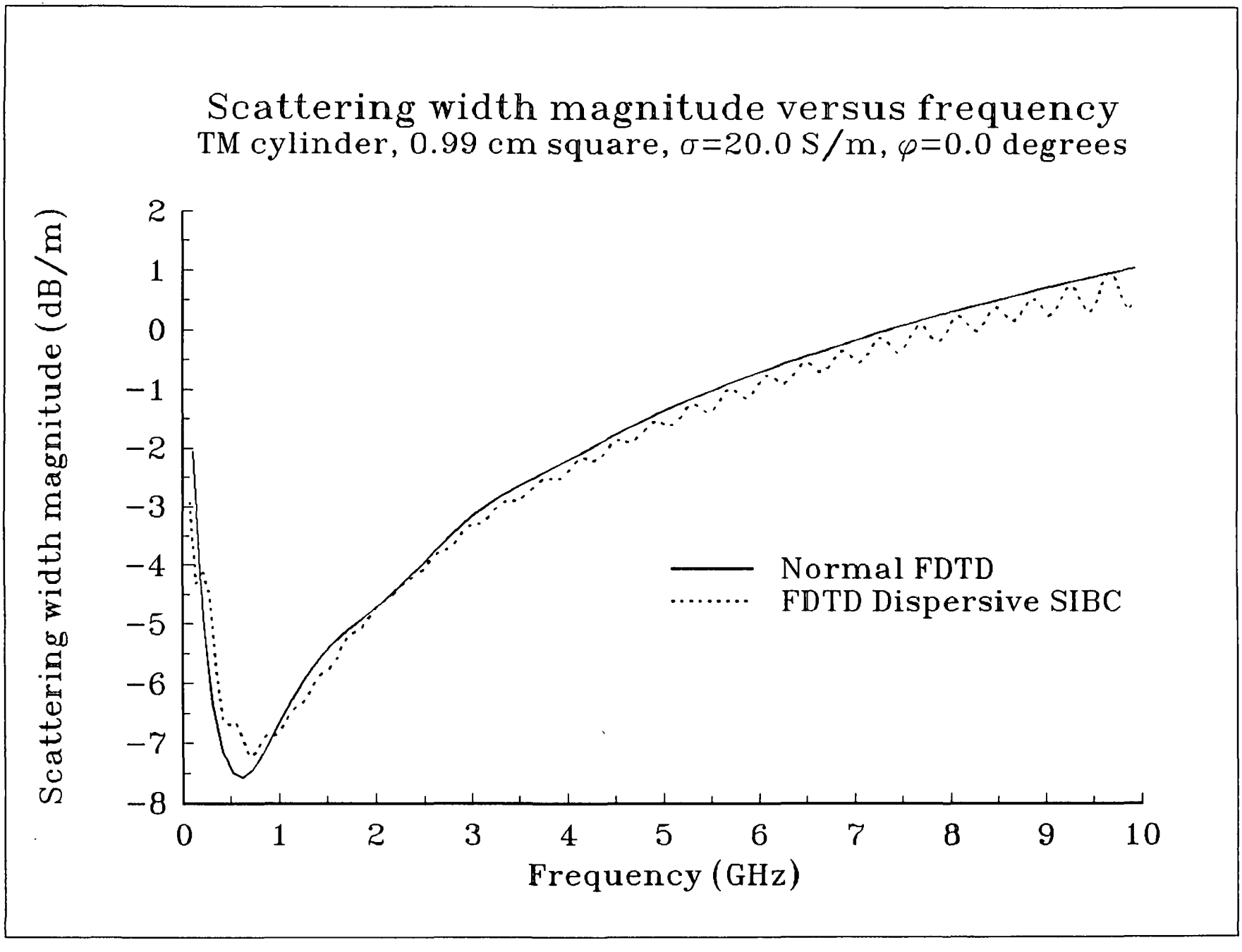
Scattering width magnitude versus frequency
TM cylinder, 0.99 cm square, σ=20.0 S/m, φ=0.0 degrees
Scattering width magnitude (dB/m)
2
1
0
−1
−2
−3
−4
−5
−6
−7
−8
0
1
2
3
4
5
6
7
8
9
10
Frequency (GHz)
Normal FDTD
FDTD Dispersive SIBC

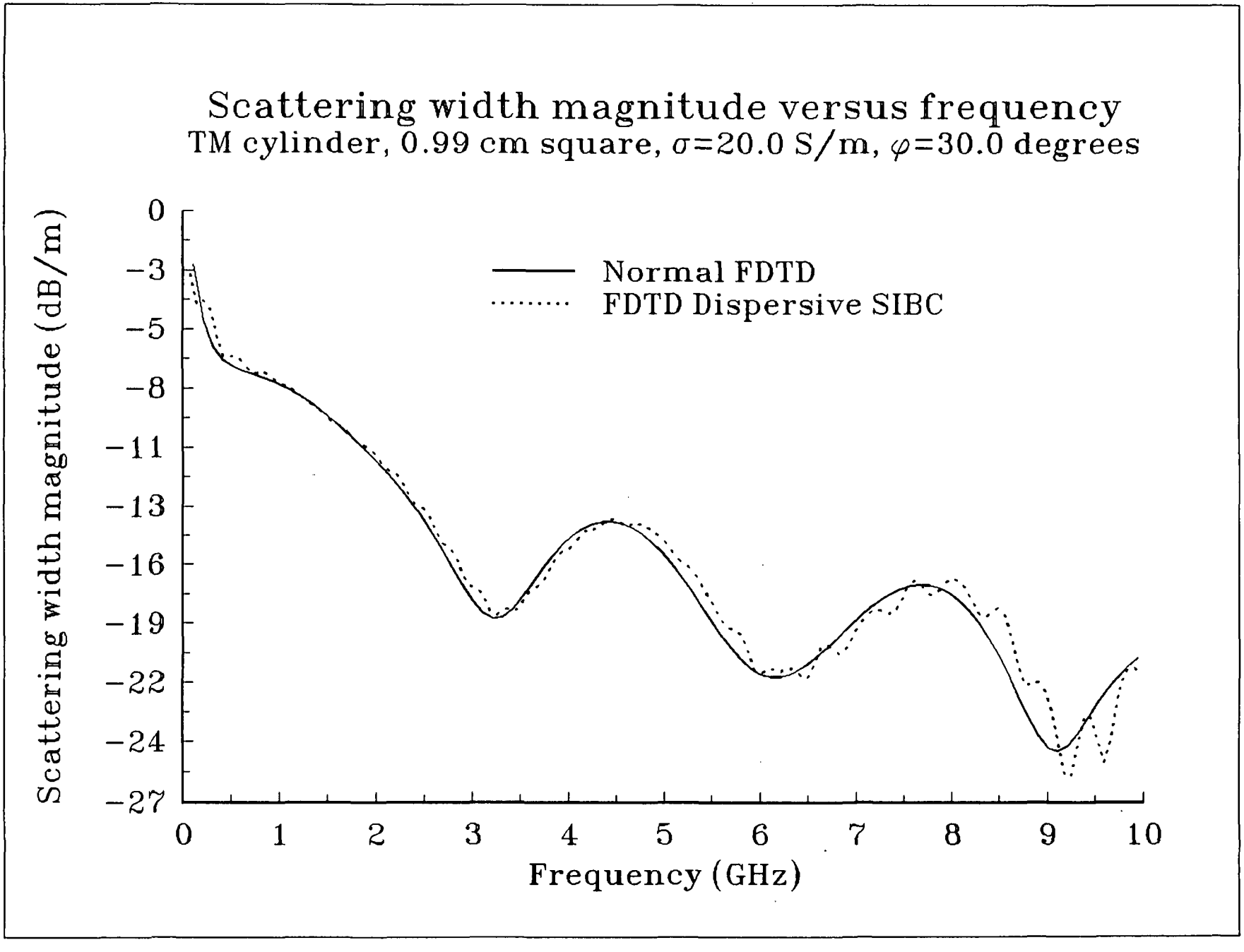
Scattering width magnitude versus frequency
TM cylinder, 0.99 cm square, σ=20.0 S/m, φ=30.0 degrees
Normal FDTD
FDTD Dispersive SIBC
Scattering width magnitude (dB/m)
0
-3
-5
-8
-11
-13
-16
-19
-22
-24
-27
0
1
2
3
4
5
6
7
8
9
10
Frequency (GHz)